Technical Reference on Hydrogen Compatibility of Materials

Austenitic Stainless Steels:
22-13-5 (code 2201)

Prepared by:
C. San Marchi, Sandia National Laboratories

Editors
C. San Marchi
B.P. Somerday
Sandia National Laboratories

This report may be updated and revised periodically in response to the needs of the technical community; up-to-date versions can be requested from the editors at the address given below. The success of this reference depends upon feedback from the technical community; please forward your comments, suggestions, criticisms and relevant public-domain data to:

Sandia National Laboratories
Matls Tech Ref
C. San Marchi (MS-9402)
7011 East Ave
Livermore CA 94550.

This document was prepared with financial support from the Safety, Codes and Standards program element of the Hydrogen, Fuel Cells and Infrastructure program, Office of Energy Efficiency and Renewable Energy; Pat Davis is the manager of this program element. Sandia is a multiprogram laboratory operated by Sandia Corporation, a Lockheed Martin Company, for the United States Department of Energy under contract DE-AC04-94AL85000.

1. General

Alloy 22-13-5 is a nitrogen-strengthened austenitic stainless steel that combines excellent corrosion resistance with high yield strength, ductility and fracture toughness at room temperature and cryogenic temperatures. Yield strengths greater than 1000 MPa can be achieved in this alloy by warm-working. Although ferrite is typically not observed in bar stock, solidification of primary ferrite is thought to be important for high quality fusion welds and is observed in welded joints.

Although very little data exist for 22-13-5 in gaseous hydrogen environments, published tensile data indicate that this alloy is not strongly affected by hydrogen gas environments even at cryogenic temperatures. This is attributed to the relatively high stacking fault energy in this alloy [1, 2], which promotes cross slip and homogeneous deformation.

1.1 Composition

Table 1.1.1 lists the UNS composition for 22-13-5 and the compositions of several heats of 22-13-5 used to study hydrogen effects.

1.2 Other Designations

Nitronic 50, XM-19, UNS S20910

2. Permeability and Solubility

Ref. [3] provides a summary of data for other stainless steels. It is important to note that permeability and solubility data are generally extrapolated from temperatures above ambient and pressures of a few atmospheres or less; as a consequence, there is a significant amount of scatter amongst the data. The temperature dependent permeability is typically expressed as

$$\phi = \phi_o \exp\left(-E_\phi / RT\right)$$

Louthan and Derrick found that a single set of constants described the permeability of deuterium in a number of austenitic stainless steels [4]; these constants are:

$$\phi_o = 1.19\text{x}10^{-4} \frac{\text{mol H}_2}{\text{m} \cdot \text{s} \cdot \sqrt{\text{MPa}}} \text{ and } E_\phi = 59.8 \text{ kJ/mol.}$$

The pre-exponential factor has been corrected to account for the difference between deuterium and hydrogen by multiplying by $\sqrt{2}$. Although the permeability of hydrogen in 22-13-5 has not been measured, these relationships provide an estimate.

The solubility of hydrogen in steels is assumed to follow Sievert's Law: hydrogen concentration in the steel is proportional to the square root of the fugacity of the hydrogen gas. The proportionality constant, Sievert's parameter (*S*) has the standard Arrhenius form:

$$S = S_o \exp\left(-E_S / RT\right)$$

The solubility in nitrogen-strengthened austenitic stainless steel appears to be about 50 to 100% higher than the 300-series stainless steels [5, 6]. Thus, the solubility in 22-13-5 is estimated here by taking the temperature dependence proposed by Louthan and Derrick [4] for a variety of austenitic stainless steels and a pre-exponential factor based on measured uniform hydrogen concentrations in 22-13-5 that have been reported in the literature [2, 6, 7]:

$$S_o = 214\,\frac{\text{mol H}_2}{\text{m}^3\cdot\sqrt{\text{MPa}}} \text{ and } E_S = 5.8 \text{ kJ/mol}$$

These values are offered as a general indicator of solubility and may not be accurate for all conditions; hydrogen concentrations quoted elsewhere in this document are values that have been reported in the respective reference. A thorough study of solubility in this alloy is needed, including analysis of the effect of composition on solubility, in particular the effect of nitrogen.

3. Mechanical Properties: Effects of Gaseous Hydrogen

3.1 Tensile properties

3.1.1. Smooth tensile properties

This alloy generally shows low degradation of tensile ductility due to hydrogen for temperatures from 77 K to 380 K. In some cases, hydrogen increased yield strength, although this effect is small. Modest decreases in strength have also been reported, although not more than 10% loss. Basic tensile properties of hydrogen-exposed 22-13-5 from a number of studies at room temperature are summarized in Table 3.1.1.1. Figure 3.1.1.1 shows the effects of both internal and external sources of hydrogen on the tensile properties of two forgings (these data are also in Table 3.1.1.1). An important exception to the trends in Table 3.1.1.1 is shown in Figure 3.1.1.2: significant ductility losses were reported for high energy rate forging (HERF) samples that were thermally precharged in hydrogen gas and then tested in high pressure hydrogen gas at room temperature. The fracture mode remained ductile, dominated by microvoid coalescence, at pressures of hydrogen up to 173 MPa, with the lowest measured RA of 35% [8]. Details of the microstructure and mechanical properties are not provided in that study.

The effect of cryogenic temperature is shown in Figure 3.1.1.3 and 3.1.1.4 for 22-13-5 thermally charged with hydrogen.

3.1.2 Notched tensile properties

This alloy shows some ductility loss due to hydrogen in notched tensile specimens precharged with high concentrations of hydrogen. The reduction of area measured in notched tensile specimens is shown in Fig. 3.1.2.1 for two heats of 22-13-5 subjected to two heat treatments in the uncharged and thermally precharged conditions. These data also demonstrate the importance of microstructural control as the loss in ductility due to heat treating at 1073 K is greater than the loss due to hydrogen exposure in material heat treated at 1273 K, see section 4.2. The fracture mode, microvoid coalescence, was not noticeably affected by precharging with hydrogen in these specimens.

Notched tensile data for cryogenic temperatures are shown in Figure 3.1.2.2; these data show less ductility loss, possibly due to lower hydrogen concentrations.

3.2 Fracture mechanics

3.2.1 Fracture toughness

The effect of hydrogen on fracture properties was found to vary substantially in forged materials depending on orientation of the propagating crack relative to the microstructure [9]. The J-integral fracture toughness at maximum load J_m and the tearing modulus at maximum load dJ/da (change in J with crack length) are more susceptible to hydrogen effects when the crack is propagating perpendicular to forging flow lines in forged bar as compared to propagating parallel to forging flow lines, Table 3.2.1.1. Even though the values of J_m and dJ/da are affected by hydrogen for cracks propagating across flow lines, the hydrogen-affected values remain greater than the values for cracks propagating along flow lines in material not exposed to hydrogen.

3.2.2 Threshold stress intensity

No crack propagation was observed in wedge-opening load (WOL) testing in hydrogen gas at a stress intensity of 132 MPa $m^{1/2}$ [10]. The material, P81 Table 1.1.1, was high-energy rate forged at 980˚C, and had a yield strength of 724 MPa. Crack propagation was nominally parallel to the flow lines of the forging. The WOL specimen was loaded in 200 MPa hydrogen gas at ambient temperature for 5000 hours. The testing procedure generally followed the requirements of ASTM E 1681-99 [11].

3.3 Fatigue

No known published data in hydrogen gas.

3.4 Creep

No known published data in hydrogen gas.

3.5 Impact

Charpy impact toughness was not affected by thermally precharging 22-13-5 (68 wppm uniform hydrogen) at room temperature and 77 K [7]. The tensile properties of the material tested in impact are given in Figure 3.1.1.4.

3.6 Disk Rupture Tests

Disk rupture tests of 22-13-5, heat A87, and other nitrogen-strengthened stainless steels display slight to moderate reductions in rupture pressure when pressurized with hydrogen compared to helium [12].

4. Fabrication

4.1 Primary processing

Microstructural features such as flow lines can have a significant effect on fracture toughness in air and in a hydrogen environment; therefore, microstructural orientation is an important design consideration.

4. 2 Heat treatment

Control of processing temperatures is important, as there is some evidence that brittle second phases can form at temperatures less than 1123 K [2]. In similar alloys such as 21-6-9, ferrite may rapidly transform to brittle σ-phase in the temperature range of about 923 K to 1173 K [13]. These microstructural issues are independent of hydrogen exposure, but could exacerbate hydrogen-assisted fracture.

4.3 Properties of welds

Detailed microstructural investigation of 22-13-5 gas tungsten arc (GTA) welds tested in hydrogen gas are presented in Ref. [14, 15]. Fracture of the welds was by microvoid coalescence and hydrogen precharging did not significantly alter the morphology of the fracture surfaces. The tensile properties are listed in Table 4.1.1.

5. References

1. BC Odegard, JA Brooks and AJ West. The Effect of Hydrogen on Mechanical Behavior of Nitrogen-Strengthened Stainless Steel. in: AW Thompson and IM Bernstein, editors. Effect of Hydrogen on Behavior of Materials. New York: TMS (1976) p. 116-125.
2. BP Somerday and SL Robinson. H- and Tritium-Assisted Fracture in N-Strengthened, Austentitic Stainless Steel. JOM - J Min Met Mater Soc 55 (2003) 51-55.
3. GR Caskey. Hydrogen Effects in Stainless Steels. in: RA Oriani, JP Hirth and M Smialowski, editors. Hydrogen Degradation of Ferrous Alloys. Park Ridge NJ: Noyes Publications (1985) p. 822-862.
4. MR Louthan and RG Derrick. Hydrogen Transport in Austenitic Stainless Steel. Corrosion Science 15 (1975) 565-577.
5. GR Caskey and RD Sisson. Hydrogen Solubility in Austenitic Stainless Steels. Scr Metall 15 (1981) 1187-1190.
6. GR Caskey. Hydrogen Damage in Stainless Steel. in: MR Louthan, RP McNitt and RD Sisson, editors. Environmental Degradation of Engineering Materials in Hydrogen. Blacksburg VA: Laboratory for the Study of Environmental Degradation of Engineering Materials, Virginia Polytechnic Institute (1981) p. 283-302.
7. L Ma, G Liang, J Tan, L Rong and Y Li. Effect of Hydrogen on Cryogenic Mechanical Properties of Cr-Ni-Mn-N Austenitic Steels. J Mater Sci Technol 15 (1999) 67-70.
8. AJ West and MR Louthan. Dislocation Transport and Hydrogen Embrittlement. Metall Trans 10A (1979) 1675-1682.
9. GR Caskey. Hydrogen Compatibility Handbook for Stainless Steels (DP-1643). EI du Pont Nemours, Savannah River Laboratory, Aiken SC (June 1983).

10. MW Perra. Sustained-Load Cracking of Austenitic Steels in Gaseous Hydrogen. in: MR Louthan, RP McNitt and RD Sisson, editors. Environmental Degradation of Engineering Materials in Hydrogen. Blacksburg VA: Laboratory for the Study of Environmental Degradation of Engineering Materials, Virginia Polytechnic Institute (1981) p. 321-333.
11. ASTM E 1681-99, Standard Test Method for Determining Threshold Stress Intensity Factor for Environment-Assisted Cracking of Metallic Materials. American Society for Testing and Materials (1999).
12. PF Azou and JP Fidelle. Very low strain rate hydrogen gas embrittlement (HGE) and fractography of high-strength, mainly austenitic stainless steels. in: MR Louthan, RP McNitt and RD Sisson, editor. Environmental Degradation of Engineering Materials III. The Pennsylvania State University, University Park PA (1987) p. 189-198.
13. CL Ferrera. The Formation and Effects of Sigma Phase in 21-6-9 Stainless Steel (PMT-87-0017). Rockwell International, Rocky Flats Plant, Golden CO (November 1987).
14. JA Brooks and AJ West. Hydrogen Induced Ductility Losses in Austenitic Stainless Steel Welds. Metall Trans 12A (1981) 213-223.
15. JA Brooks, AJ West and AW Thompson. Effect of Weld Composition and Microstructure on Hydrogen Assisted Fracture of Austenitic Stainless Steels. Metall Trans 14A (1983) 75-84.
16. ASTM. Metals and Alloys in the UNIFIED NUMBERING SYSTEM (SAE HS-1086 OCT01; ASTM DS-56H). Society of Automotive Engineers; American Society for Testing and Materials, (2001).
17. BC Odegard and AJ West. On the Thermo-Mechanical Behavior and Hydrogen Compatibility of 22-13-5 Stainless Steel. Mater Sci Eng 19 (1975) 261-270.
18. TL Capeletti and MR Louthan. The Tensile Ductility of Austenitic Steels in Air and Hydrogen. J Eng Mater Technol 99 (1977) 153-158.

Table 1.1.1. Composition of several heats of 22-13-5 used to study hydrogen effects as well as specification limits.

heat	Fe	Cr	Ni	Mn	Mo	Si	C	N		Ref.
UNS S20910	Bal	20.50 23.50	11.50 13.50	4.00 6.00	1.50 3.00	1.00 max	0.06 max	0.20 0.40	0.10-0.30 Nb; 0.10-0.30 V; 0.030 max S; 0.060 max P	[16]
O75	Bal	22.15	12.74	5.26	2.20	0.50	0.050	0.34	0.23 Nb; 0.26 V; 0.006 S; 0.019 P	[17]
O76	Bal	23.00	12.98	4.68	1.75	0.36	0.050	0.38		[1]
P81	Bal	23.11	12.91	4.76	1.75	0.38	0.05	0.39	0.18 Nb	[10]
C83	Bal	21.48	12.36	5.44	2.12	0.42	0.05	0.25	0.19 Nb; 0.2 V; 0.010 S; 0.015 P	[9]
B83*	Bal	22.9	12.9	4.6	1.8	0.42	0.05	0.35	0.008 S; 0.012 P	[15]
A87	Bal	21.6	12.2	5.1	2.1	0.38	0.051	0.27	0.007 S; 0.02 P	[12]
S03a	Bal	21.26	11.87	4.67	2.20	---	0.036	0.276		[2]
S03b	Bal	21.32	13.11	5.02	2.04	---	0.013	0.30		[2]

* composition in GTA weld fusion zone

Table 3.1.1.1. Tensile properties of 22-13-5 thermally precharged and tested in hydrogen gas at room temperature.

Material	Thermal precharging	Test environment	Strain rate (s^{-1})	S_y (MPa)	S_u (MPa)	El_u (%)	El_t (%)	RA (%)	Ref.
Bar, as-received, heat C83	None	Air	---	440	710	---	43	72	[6, 9, 18]
	None	69 MPa He		400	680	---	47	74	
	None	69 MPa H_2		400	680	---	45	73	
Bar, as-received	None	Air	---	800*	1190†	32	41	69	[9]
	(1)	Air		820*	1240†	33	44	65	
Annealed plate, heat O76	None	Air	3 $x10^{-3}$	586	938	---	51	67	[1]
	(2)	69 MPa H_2		579	951	---	54	68	
Warm-worked bar, heat O75	None	Air	0.3 $x10^{-3}$	841	958	30	---	66	[17]
	None	69 MPa H_2		841	986	27	---	67	
	(2)	Air		855	1007	27	---	64	
	(2)	69 MPa H_2		924	1082	23	---	62	
High energy rate forging (HERF), heat O75	None	Air	0.3 $x10^{-3}$	1269	1317	9	---	20	[17]
	None	69 MPa H_2		1202	1276	7	---	29.5	
	(2)	Air		1262	1310	10	---	15.5	
	(2)	69 MPa H_2		1310	1365	10	---	20	

* true stress at 5% strain
† true stress at maximum load
(1) 69 MPa hydrogen gas, 620 K, 3 weeks
(2) 24 MPa hydrogen gas, 473 K, 10.5 days: calculated surface concentration of ~50 wppm hydrogen (~2500 appm)

Table 3.2.1.1. Fracture toughness parameters for 22-13-5 tested in high-pressure hydrogen gas. Note: thermal precharging was performed with deuterium gas.

Material	Thermal precharging	Test environment	J_m (kJ/m^2)	dJ/da (MPa)	Ref.
High energy rate forging (HERF) bar, parallel†	None	69 MPa He	32	176	[9]
	None	69 MPa H_2	23	137	
	(1)	69 MPa H_2	33	211	
HERF bar, perpendicular†	None	69 MPa He	936	360	[9]
	None	69 MPa H_2	107	209	
	(1)	69 MPa H_2	181	264	

† Precracked C-shaped specimens were machined from forged bar in an orientation such that the crack propagated nominally parallel to flow lines in the bar cross section, and 90˚ from this orientation such that the crack propagated nominally across (or perpendicular to) the forging flow lines.
(1) 69 MPa deuterium gas, 620K, 3 weeks

Table 4.1.1. Smooth tensile properties of 22-13-5 composite GTA weld specimens† thermally precharged with hydrogen and tested in gaseous hydrogen at room temperature. All data are provided for completeness, but it should be emphasized that these data may not reflect the properties of any of the specific microstructures within the gauge length. [15]

Thermal precharging	Test environment	Strain rate (s^{-1})	S_y (MPa)	S_u (MPa)	El_u (%)	El_t (%)	RA (%)
None	Air	0.33×10^{-3}	495	782	11.2	14.4	49
	69MPa H_2		511	778	13.0	16.3	48
	172MPa H_2		528	798	11.8	16.0	50
(1)	Air		510	789	9.6	10.9	38
	69MPa H_2		531	776	10.2	12.0	45
(2)	Air		514	789	9.9	10.7	35
	172MPa H_2		516	780	11.6	13.5	35

† The base material for these studies was HERF (high energy rate forging), back extrusions of 22-13-5, machined to hollow cylindrical shape (10 cm diameter, 1.5 cm wall thickness) with circumferential double J grooves. The filler material was also 22-13-5 matched to the composition of the base metal. Eight to ten weld passes were required and the composition of the weld fusion zone, heat B83, is given in Table 1.1.1. The tensile specimens contain base material and heat affected zone with the fusion zone centered in the gauge length.
(1) 24 MPa H_2 473K, 10 days: hydrogen concentration was calculated to vary from 45 to 4 wppm (2500 to 200 appm) surface to center.
(2) 69 MPa H_2 473K, 10 days: hydrogen concentration was calculated to vary from 73 to 7 wppm (4000 to 400 appm) surface to center.

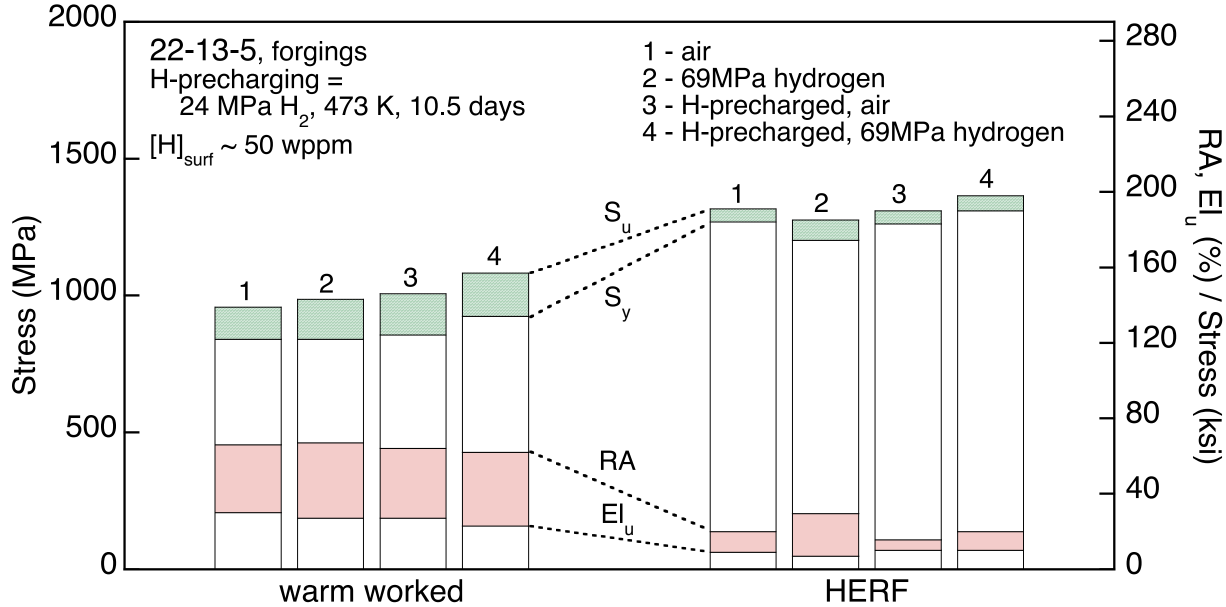

Figure 3.1.1.1. Effect of internal and external hydrogen on the tensile properties of 22-13-5 forgings (heat O75); same data is contained in Table 3.1.1.1. Strain rate = 3 x 10^{-4} s^{-1}. HERF = high energy rate forging. [17]

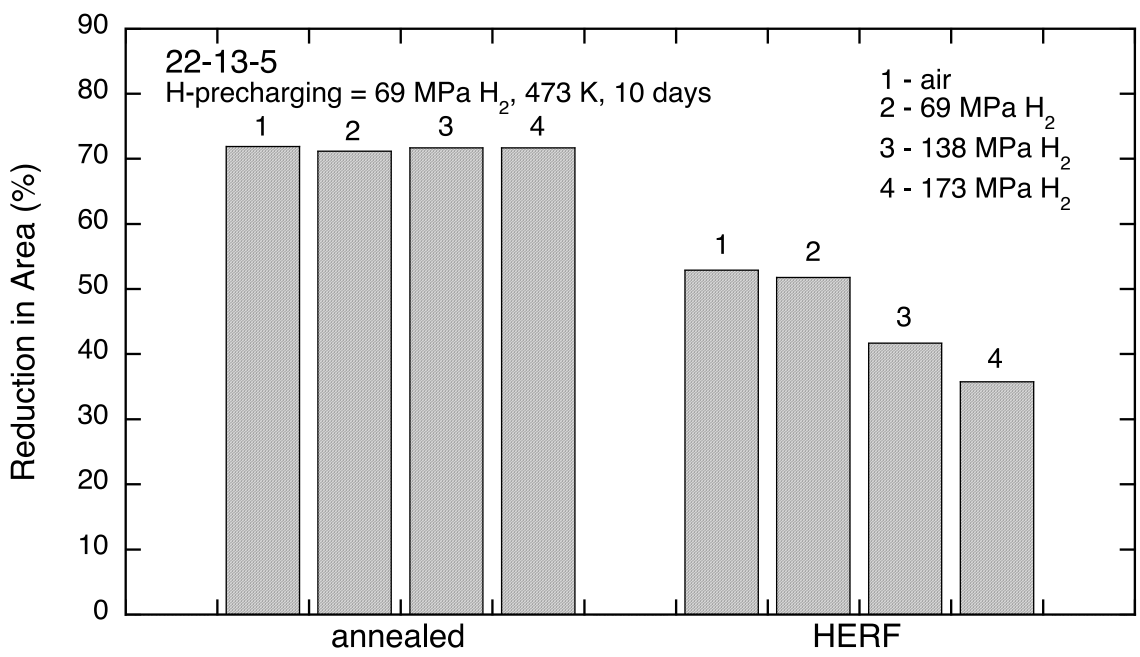

Figure 3.1.1.2. Ductility of smooth tensile specimens of annealed and forged 22-13-5 that have been precharged from hydrogen gas at elevated temperature and then tested in hydrogen gas at room temperature. HERF = high energy rate forging. [8]

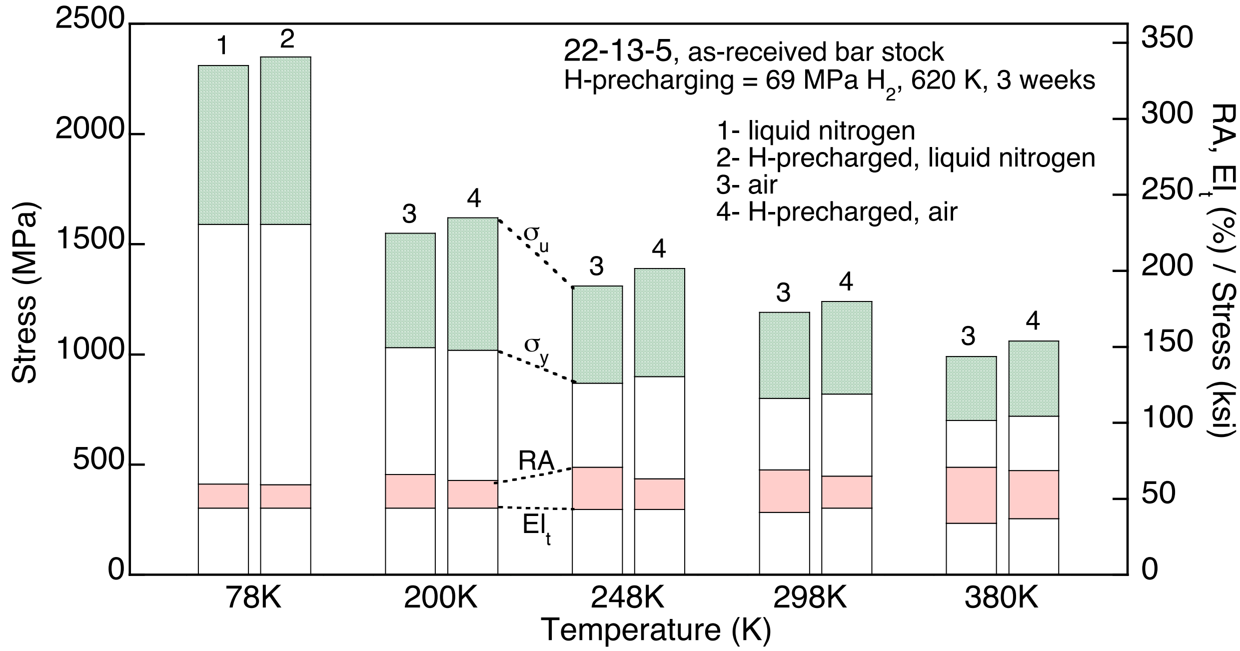

Figure 3.1.1.3. Effect of temperature on the hydrogen compatibility of 22-13-5 bar stock. Yield strength in this plot is defined as the true stress at 5% strain, ultimate strength is quoted as true stress at maximum load. [9]

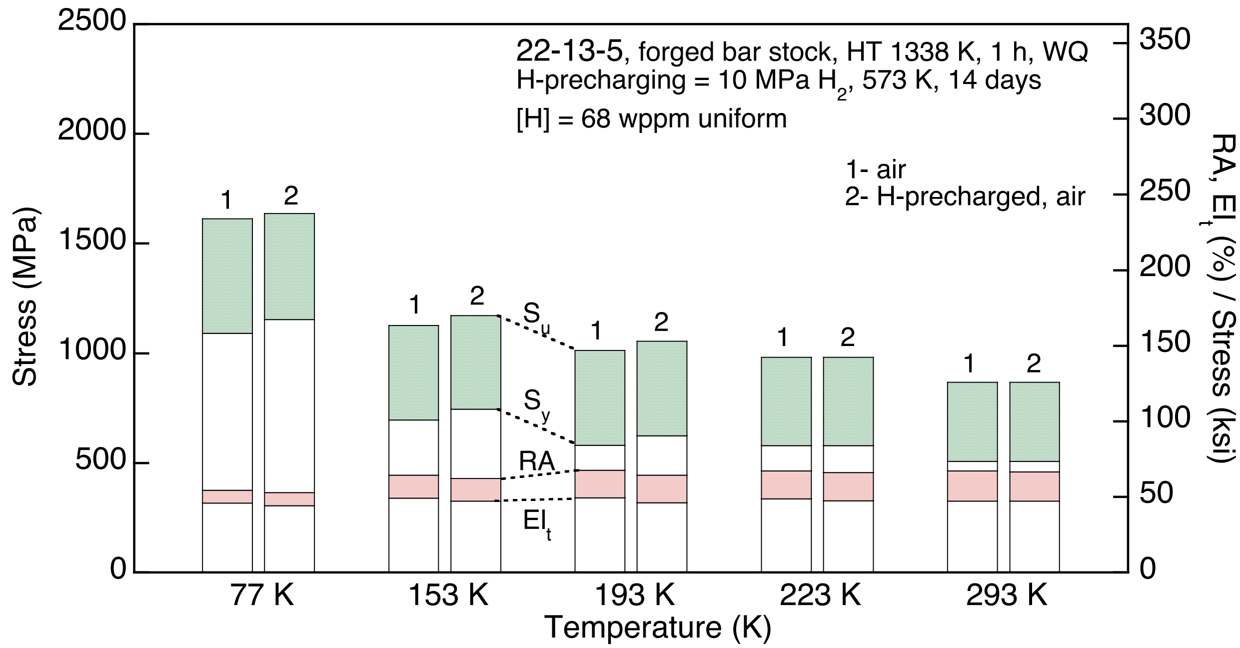

Figure 3.1.1.4. Effect of temperature on the hydrogen compatibility of 22-13-5 heat-treated bar stock. Specimen diameter = 5 mm; crosshead rate = $4.2x10^{-2}$ mm/s. HT = heat treatment, WQ = water quench. [7]

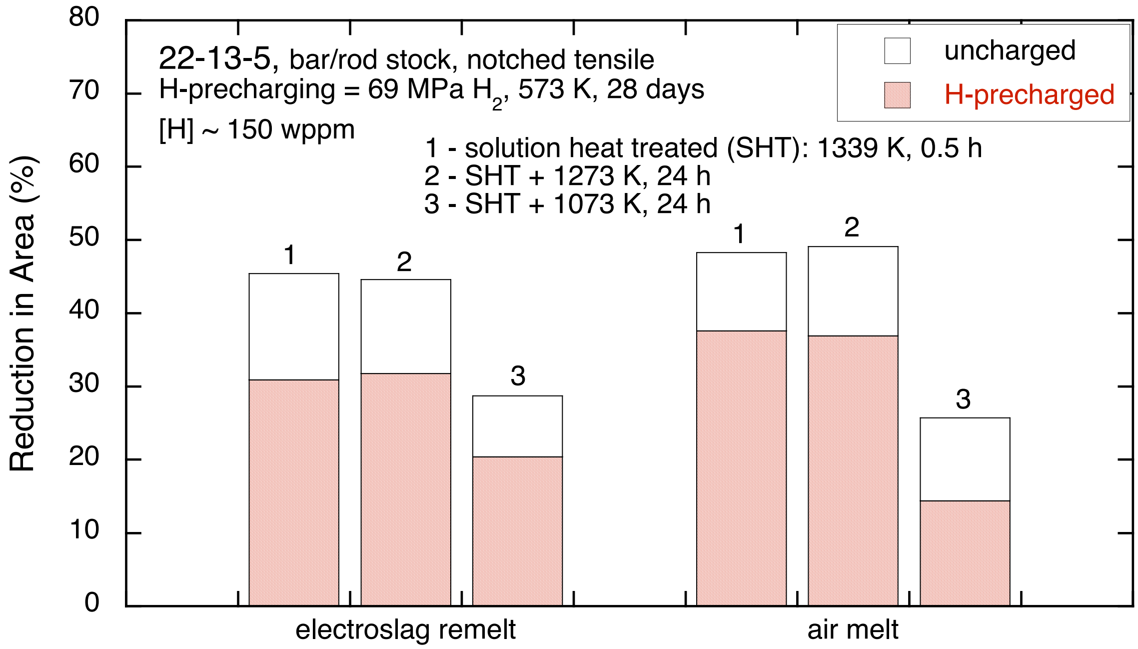

Figure 3.1.2.1. Reduction in area of notch tensile bars from two heats of 22-13-5 (electroslag remelted, heat S03b; air-melted, heat S03a). Notched specimen: semicircular notch; minimum diameter = 3.9 mm; maximum diameter = 7.9 mm; notch root radius = 0.79 mm; constant rate of displacement = 6×10^{-3} mm/s. [2]

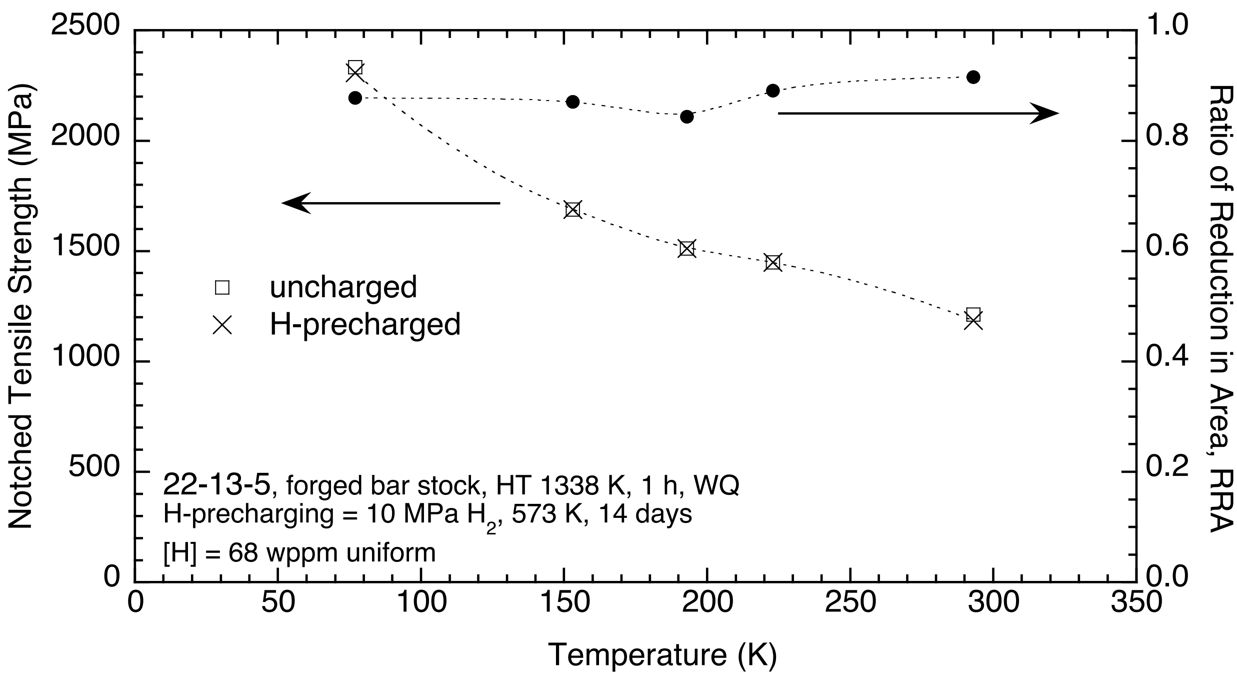

Figure 3.1.2.2. Notch tensile properties of 22-13-5 heat-treated bar stock. Notched specimen: stress concentration factor (K_t) = 4.55; notch geometry = 60° included angle; minimum diameter = 4 mm; maximum diameter = 5 mm; notch root radius = 0.1 mm; crosshead rate = 4.2×10^{-2} mm/s. HT = heat treatment, WQ = water quench. [7]